Stabilization Effect of Single-Walled Carbon Nanotubes on the Functioning of Photosynthetic Reaction Centers

Márta Dorogi,[†] Zoltán Bálint,[‡] Csilla Mikó,[§] Bertrand Vileno,[§] Mirko Milas,[§] Klára Hernádi,[||] László Forró,[§] György Váró,[‡] and László Nagy*,[†]

Institute of Medical Physics and Biophysics, University of Szeged, Szeged, Hungary, Institute of Biophysics, Biological Research Center, Szeged, Hungary, Institute of Physics of Complex Matter, Ecole Polytechnique Fédérale de Lausanne, CH-1015 Lausanne, Switzerland, Department of Applied and Environmental Chemistry, University of Szeged, Szeged, Hungary

Received: February 8, 2006; In Final Form: August 21, 2006

The interaction between single-walled carbon nanotubes and photosynthetic reaction centers purified from purple bacterium *Rhodobacter sphaeroides* R-26 has been investigated. Atomic force microscopy studies provide evidence that reaction center protein can be attached effectively to the nanotubes. The typical diameter of the nanotube is 1−4 nm and 15 ± 2 nm without and with the reaction centers, respectively. Light-induced absorption change measurements indicate the stabilization of the $P^+(Q_AQ_B)^-$ charge pair, which is formed after single saturating light excitation after the attachment to nanotubes. The separation of light-induced charges is followed by slow reorganization of the protein structure. The stabilization effect of light-initiated charges by the carbon nanotubes opens a possible direction of several applications, the most promising being in energy conversion and storage devices.

1. Introduction

The one-dimensional structural and electronic properties of carbon nanotubes have made them suitable candidates for the promotion of heterogeneous electron-transfer studies, in which delicate biomolecules "communicate" with the interface of electric circuits. There is convincing evidence that nanotubes are very efficient components in devices based on biomatter. For example, bioelectrochemical reactions can be driven by attaching small proteins to the surface of carbon nanotubes.[1,2] Well-controlled aligned carbon nanotubes can be applied as immobilization matrixes and as mediators for the development of third-generation amperometric biosensor devices.[3] It was found that the protein structure and function were highly influenced by the nanoscale environment. Thirty percent of the activity of the soybean peroxidase and only 1% of the activity of the α-chymotrypsin remained if these proteins were bound to single-walled carbon nanotubes.[4]

This work is the first to show experiments carried out with photosynthetic reaction center (RC) pigment protein complex, the well-known redox-active enzyme in which light energy initiates a chain of intraprotein electron transport reactions attached to single-walled carbon nanotubes (SWNT). The RC is a pigment−protein system in which the primary steps of the photoelectronic energy conversion take place during photosynthesis. The capture of light energy by bacteriochlorophylls in photosynthetic bacteria is followed by separation of positive and negative charges in the state of P^+BPheo^- then $P^+Q_A^-$. Here P^+ is the oxidized primary donor, a specialized bacteriochlorophyll dimer, $(BChl)_2$, BPheo is the first electron acceptor, a monomer bacteriopheophytin, and Q_A^- is the reduced quinone-type primary electron acceptor. The separated charges are then further stabilized in form of a $P^+Q_B^-$ redox state, where Q_B^- is the reduced secondary quinone (Figure 1, for reviews see, e.g., refs 5−9). Although the quantum efficiency of the primary charge separation is close to one in RC,[10] the physical parameters of the electron transport depend on the type of the RC and on the environmental factors. Specific molecules (such as detergents, lipids, inhibitors, etc.) bind to specific sites of the RCs of purple bacteria,[11−14] thus they modify the kinetics and energetics of the charge stabilization.

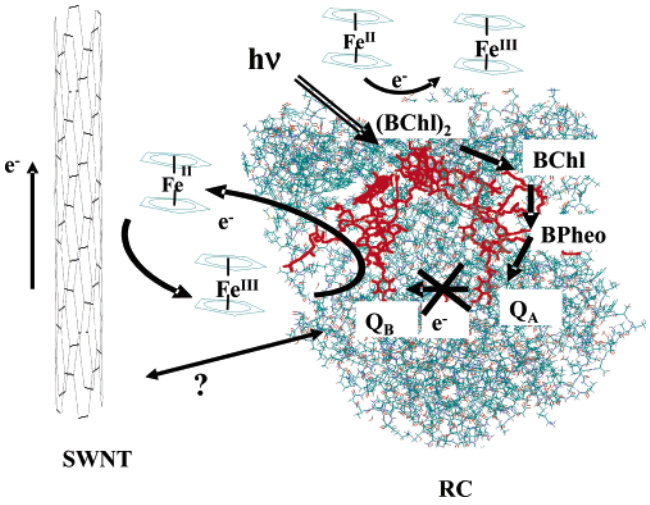

Figure 1. Schematic presentation of the positions of cofactors and the path of the electron flow in the RC protein and of the possible interaction between the carbon nanotube and the RC. X indicates the electron transport step, which is blocked by the inhibitor, terbutryn.

Our goal is to show that SWNT bound to RC serve not only as perturbation, but as entities which stabilize the RC photochemistry even in dry form. Furthermore, they should play the role of electrodes, which evacuate the photoexcited electrons.

* Corresponding author. E-mail: lnagy@sol.cc.u-szeged.hu.
[†] Institute of Medical Physics and Biophysics, University of Szeged.
[‡] Institute of Biophysics, Biological Research Center.
[§] Institute of Physics of Complex Matter.
[||] Department of Applied and Environmental Chemistry, University of Szeged.

10.1021/jp060828t CCC: $33.50
Published on Web 10/06/2006

2. Experimental Section

2.1. Sample Preparations. *Rb. sphaeroides* R-26 cells were grown photoheterotrophically.[15] RCs were prepared by LDAO (*N*,*N*-dimethyldodecylamine-*N*-oxide, Fluka) solubilization and purified by ammonium sulfate precipitation, followed by DEAE Sephacel (Sigma) anion-exchange chromatography.[16] After preparation, the RC Q_B site was reconstituted by the addition of ubiquinone-10 (UQ-10) and concentrated by centrifuge filter (Whatman VectaSpin 3, 10 kDa exclusion) to 80−100 μM. For optical spectroscopy, the RC suspension was diluted to 1 μM in detergent suspension (10 mM TRIS, 100 mM NaCl, 0.01% LDAO, pH 8.0). To bind RCs to SWNTs, 500 μL of purified RCs were incubated with the suspension of SWNT and subjected to intensive dialysis against 750 cm^3 distilled water for 3 days. The distilled water was changed and the suspension was sonicated in a water bath (10 s continuously, ELMA Transsonic 310) every 12 h. The RC concentration was kept as high as possible, routinely 80−100 μM. The mass-to-mass ratio was routinely 10 ± 3 mg RC/mg SWNT. After the dialysis, the sample was sedimented by ultracentrifuge (100 000 × g, 20 min, SORVALL ULTRA Pro, A-1256 rotor), and the precipitate was suspended in distilled water by sonication for 10−20 s. The supernatant was checked for the unbound RCs, and the resuspended precipitate was subjected to second ultracentrifugation. Finally, the precipitate was resuspended in about 500 μL of distilled water, and few drops of sample were dried onto a glass surface under a N_2 stream, and then the optical characteristics were measured. For measuring the appearance and disappearance of the semiquinone absorption, the dried sample was immersed in TRIS buffer (10 mM TRIS, 100 mM NaCl, pH 8.0) in a spectroscopic cuvette and treated by 100 μM ferrocene. For inhibition of the secondary quinone site, terbutryn was added at a concentration of 400 μM. Ferrocene and terbutryn were added from ethanolic stock solutions of 100 mM and 50 mM, respectively. The amount of the ethanol in the sample after the chemical treatment was about 1%, which did not have an observable affect on the RC photochemistry.

2.2. Origin and Purification of SWNT. Commercially available SWNTs, produced by a high-pressure CO process (HiPco), have been purchased from Carbon Nanotechnologies Incorporated Company and were purified by wet oxidation technique. Raw HiPco SWNTs (100 mg) were oxidized in a mixture of 60 mL of 30% H_2O_2 and 110 mL of 22% HCl.[17] The suspension was then refluxed under continuous magnetic stirring at 70 °C for 9 h. Then it was cooled to room temperature, and SWNTs were filtered and washed with distilled water until pH 7. Finally, SWNTs were dried at 120 °C for 30 min. The yield of purified SWNTs was 90%, determined by transmission electron microscopy. The average diameter of the tubes is 1.5 nm.

2.3. Optical Spectroscopy. Flash-induced absorption changes were measured routinely by a single-beam kinetic spectrophotometer of local design.[16,18,19] The P/P^+ redox changes of the primary bacteriochlorophyll dimer,[16,20] the electrochromic response of the absorption of bacteriopheophytins to the formation of the $Q_A^-Q_B$ and $Q_AQ_B^-$ states,[21] and the appearance and disappearance of the semiquinone species[16] were detected at 860 or 430, 771, and 450 nm, respectively. The apparent one-electron equilibrium constant in the acceptor quinone complex, $K_{AB} = [Q_AQ_B^-]/[Q_A^-Q_B]$ was determined from the rate of the fast (k_f) and slow (k_s) components of the $P^+(Q_AQ_B)^- \rightarrow PQ_AQ_B$ charge recombination in the dark: $K_{AB}^{app} = k_f/k_s - 1$. The free energy gap between $Q_A^-Q_B$ and $Q_AQ_B^-$ states is $\Delta G_{AB}^0 = -k_B \cdot T \cdot \ln K_{AB}^{app}$, where k_B and T are the Boltzmann constant and the absolute temperature, respectively.[22,23]

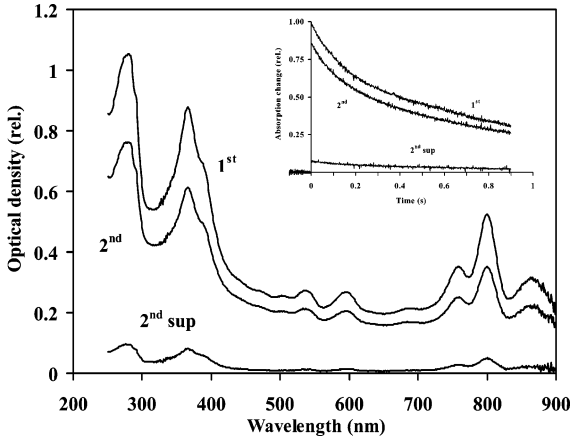

Figure 2. Spectra of the fractions of SWNTRC samples after the first, 1st, and second, 2nd, run with the ultracentrifuge. "2ndsup" indicates the spectrum of the supernatant sample after the second centrifugation. Insert indicates the flash-induced absorption changes of the same samples measured at 430 nm.

2.4. Atomic Force Microscopy. Sample preparation: The SWNT/RC, RC, and SWNT suspension was dried on freshly cleaved Muscovite mica (SPI Supplies Division, West Chester, PA), glued to a microscope glass slide. Images were taken with an MFD-3D atomic force microscope (Asylum Research, Santa Barbara, CA). The scanning was performed in AC (tapping) mode with an Olympus cantilever AC160 (Tokyo, Japan) having a nominal force constant about 40 N/m and resonance frequency of about 325 kHz. The images were made with a scan frequency of 2 lines/s and digitized in 512 × 512 pixels.

2.5. EPR Spectroscopy. A small quantity of the RC and SWNT/RC complexes was dried on a glass surface under a N_2 stream. A fraction of the obtained films (1−3 mm^2) of SWNT/RC and the RC samples were loaded subsequently into a suprasil tube of 5 mm and introduced into an standard TE_{102} EPR cavity of a Bruker ESP300E X-band spectrometer. The sample was illuminated with white light (80 W source) through an optical fiber, which was coupled to the tube from the top. The magnetic field was fixed at the value where the EPR signal had its peak in intensity, both for RC and SWNT/RC. Scan conditions were as follows: microwave frequency, 9.39 GHz, power 2mW, modulation amplitude 1.0 G, modulation frequency 100 kHz, and center field at 3342 G. The signal was recorded in time with on−off sequences of illumination of 1 min. All experiments were performed at ambient temperature.

3. Results

3.1. Binding RCs to the Carbon Nanotubes. *Optical Studies.* Because, during the usual purification procedure the pure RC is separated by 240 000 × g, it can be expected that after running the ultracentrifuge at 100 000 × g, only the unbound RCs are found in the supernatant. After ultracentrifugation, the absorption spectrum of the supernatant and the resuspended precipitate was measured. The spectrum shows all of the absorption peaks, which are characteristic of the photosynthetic reaction centers. The change in the baseline is caused by the light scattering due to the presence of carbon nanotubes. Figure 2 obviously shows that, after the second run in the ultracentrifuge under the same conditions, the overwhelming part of RCs remained in the precipitate attached to the nanotubes. Flash-induced change in the absorption at 430 nm (Figure 2, insert) indicates that RCs kept their photosynthetic

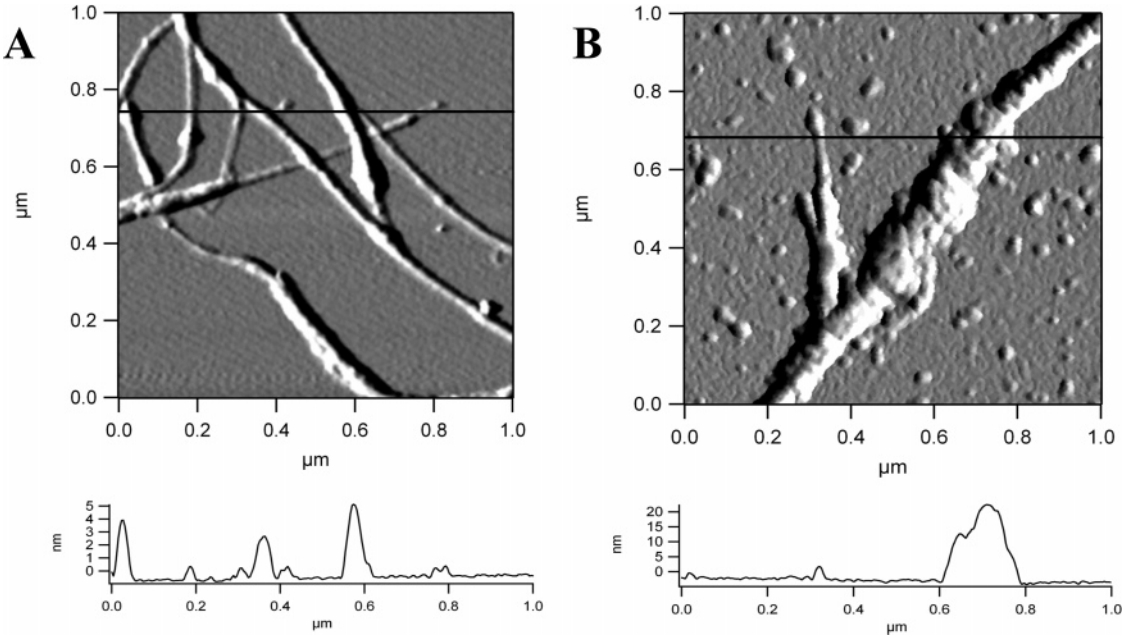

Figure 3. Amplitude image and section of the height image of single-walled nanotubes (A) and the photosynthetic reaction centers sitting on single-walled carbon nanotube (B). Original scan size is 1 μm for the SWNTs and for the SWNT/RC complex. The average height of the RC, the SWNT, and SWNT/RC complex is 9 ± 1 nm, 1−4 nm, and 15 ± 2 nm, respectively.

activity after binding to carbon tubes. The ratio of the amplitudes of the signals indicated that approximately 85% of the active RCs were bound to the carbon nanotubes.

Atomic Force Microscope Studies. A few drops of the sample were dried onto freshly cleaved mica for structural characterization by atomic force microscopy (AFM). Figure 3 shows that the average diameter (indicated in the amplitude image section) of the RC, the SWNT, and SWNT/RC complex is 9 ± 1 nm, 1−4 nm, and 15 ± 2 nm, respectively. This comparison clearly shows that there is an effective binding of RC to single-walled carbon nanotubes. SWNT is covered by huge amount of RCs and there are only short distances that are uncovered. The image in Figure 3 is also an example for representing the exceptional situation that, in some rare cases, there are two layers of RCs around the nanotubes.

3.2. Kinetics and Energetics of Charge Stabilization in Single Turnover. To learn more about the charge dynamics in the SWNT/RC complex, optical spectroscopy measurements were performed. Two kinds of experiments can be carried out. Without an externally added electron donor to P^+, the RC performs a single turnover after light excitation and can be excited again only after charge recombination. In a second arrangement, the RC is reset by a secondary donor to P^+ so that a multiple turnover can be investigated. To the first approach, the kinetics of various electron-transfer reactions, and the changes in the energetics of the acceptor quinone system, can be followed by the applied assays. We understand that additional experiments are needed to describe these physical parameters in detail, which are beyond the aims of this introductory work.

Charge Recombination Studies. Figure 4 (upper panel) shows the kinetics of absorption changes measured at 860 nm induced by single saturating light excitation of RCs dried onto the surface of glass either bound (SWNTRC_dried) or unbound (RC_dried) to the single-walled carbon nanotubes with or without detergent (see Experimental Section).

The response is analyzed in terms of the first-order kinetic rate equation $A(t) = A_i \exp(-k_i t)$, which helps to detect multicomponent relaxations and their weight in the overall

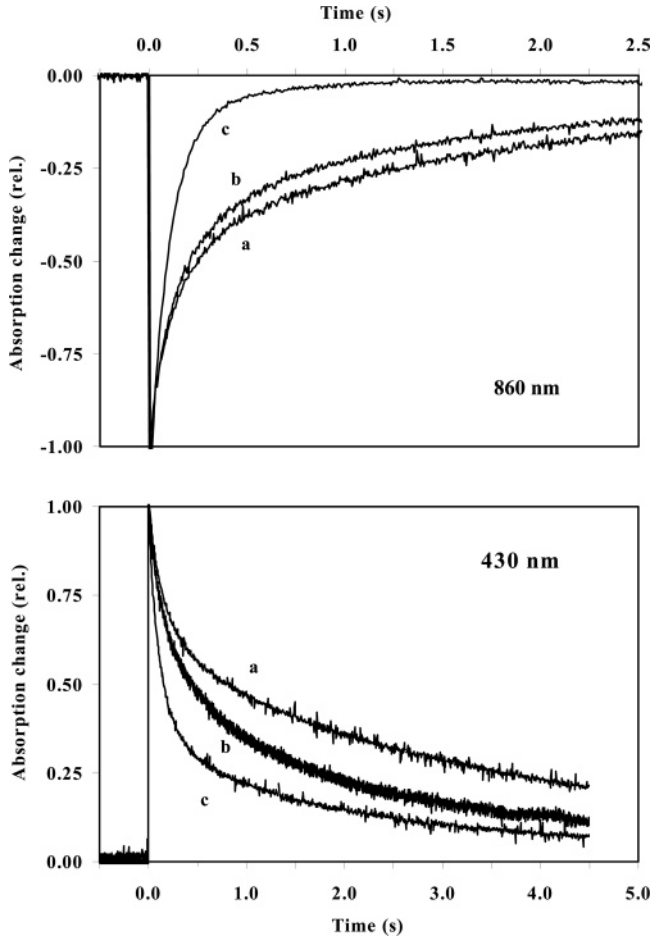

Figure 4. Kinetics of flash-induced absorption change of RCs of *Rb. sphaeroides* R-26 attached to single-walled carbon nanotubes detected at 430 nm (bottom) and 860 nm (top). SWNT/RC complex and unbound RCs were dried on the surface of borosilicate glass plate. (a) RC in LDAO detergent micelles (RC_susp); (b) RC without detergent dried immediately after deposition (RC_driedNodet_0_day); (c) RC with LDAO detergent dried immediately after deposition (RC_driedLDAO 0_day). Kinetics parameters are summarized in Table 1.

TABLE 1: Kinetic Parameters of Decomposition of the Absorption Change Kinetics at 860 and 430 nm Associated with the $P^+Q_A^-Q_B \rightarrow PQ_AQ_B$ (k_{AP}) and $P^+Q_AQ_B^- \rightarrow PQ_AQ_B$ (k_{BP}) Charge Recombination (Figure 4)[a]

	860 nm				430 nm			
	A_1 (%)	k_{BP} (s^{-1})	A_2 (rel)	k_{AP} (s^{-1})	A_1 (%)	k_{BP} (s^{-1})	A_2 (%)	k_{AP} (s^{-1})
RC_susp	95.0	0.87	5.0	8.30	87.0	0.67	13.0	8.3
RC_driedLDAO_0_day	8.0	1.15	92.0	9.66	34.0	0.39	66.0	8.3
RC_driedLDAO_1_day					3.0	0.52	97.0	8.3
RC_driedNodet_0_day	64.0	0.44	36.0	8.00	51.0	0.41	49.0	8.00
SWNTRC_0_day	43.0	0.37	57.0	6.13	59.0	0.23	41.0	4.7
SWNTRC_1_week	33.0	0.37	67.0	5.57	52.0	0.23	48.0	4.6

[a] RCs of *Rb. sphaeroides* R-26 were incorporated into LDAO detergent suspension (RC_susp), dried on the surface of borosilicate glass with (RC_driedLDAO_0_day and RC_driedLDAO_1_day) and without detergent (RC_driedNodet_0_day), and attached to single-walled nanotubes, then dried on the glass (SWNTRC_0_day and SWNTRC_1_week). In the case of RC_driedLDAO_1_day and SWNTRC_1_week, the sample was measured 1 day or 1 week later, respectively. *A* (%) and *k* are the relative amplitude (in the percentage of that of the total signal) and the rate constants of the components, respectively. The maximum error of the measurement was smaller than 10%.

response. As the turnover of the RC should involve all reactions of the bioenergetic cycle, the slowest component will determine the overall turnover rate. The index i = AP (or BP) corresponds to the $P^+Q_A^-Q_B \rightarrow PQ_AQ_B$ (k_{AP}) or to the $P^+ Q_AQ_B^- \rightarrow PQ_AQ_B$ (k_{BP}) charge recombination.[16]

At 860 nm, the redox state of the primary electron donor $(BChl)_2$ dimer, i.e., the formation and/or disappearance of P^+ after the flash excitation can be followed in a single turnover. In detergent suspension, the signal decay was almost monophasic with the rate of $k_{BP} = 0.87$ s^1 (data are summarized in Table 1). The contribution of the fast phase, $k_{AP} = 8.3$ s^{-1}, was less then 5%, indicating the slow charge recombination mainly between the P^+ and Q_B^-. When the RCs were dried on the glass from a detergent suspension, the contribution of the slow component decreased considerably. In this sample more than 90% of the fast phase was measured probably via the fast $P^+Q_A^- \rightarrow PQ_A$ process. Interestingly, if the detergent was dialized out before the deposition, the contribution of the fast phase was about 36% of the total amplitude and the rate of the slow phase reduced (from $k_{BP} = 0.87$ s^{-1} in detergent to $k_{BP} = 0.44$ s^{-1}) considerably.

When the RCs were bound to single-walled carbon nanotubes and dried on the glass surface, the decay kinetics were highly biphasic and the system was stable for several weeks. Immediately after the preparation, the rate of the slow component decreased from $k_{BP} = 0.87$ s^{-1} to $k_{BP} = 0.37$ s^{-1} ,with about 50% contribution to the total signal (Table 1). It is worthwhile to note that, in the dried samples without the detergent, there is no large difference in the rates of the slow phases ($k_{BP} = 0.44$ s^{-1} and $k_{BP} = 0.37$ s^{-1}), but the contribution of this phase is about 20% smaller in the SWNT/RC sample (64.0% compared to 43.0%).

Results were similar if the kinetics were recorded at 430 nm (Figure 4, lower panel). The parameters of the decay of charge recombination in RC suspension were practically identical to those measured at 860 nm. Also, the contribution of the slow component decreased dramatically after drying the sample onto the glass surface up to about 30%. This component disappeared completely after 24 h incubation time. In the RC dried samples without the nanotubes, the rates of the slow phases were practically identical ($k_{BP} = 0.39$ s^{-1} and $k_{BP} = 0.41$ s^{-1}). In the case of SWNTRC_dried sample, similar to the 860 nm case, a large contribution, ca. 60%, of the slow component, was measured. The rate of this decay phase slowed considerably, $k_{BP} = 0.23$ s^{-1}.

Electrochrome Shift of Bacteriopheophytine Absorption. The appearance of positive and/or negative charges induces movements of the amino acid side chains and rearrangement of hydrogen bonding or electrostatic network inside the protein.

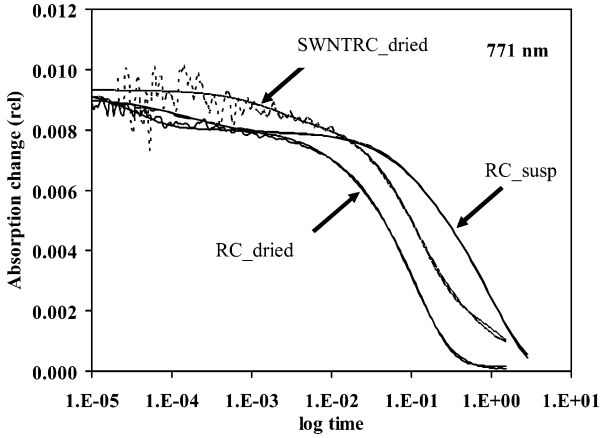

Figure 5. Absorption change of RCs of *Rb. sphaeroides* R-26 dried on the surface of borosilicate glass plate, RC_dried, and attached to SW carbon nanotubes, SWNTRC_dried, after single saturating laser flash excitation measured at 771 nm. The measured curve of RC detergent suspension, RC_susp, is also indicated. Solid lines are best fits with values listed in Table 2.

The fast charge movements are accompanied by a slower protein relaxation. To see the change in the protein relaxation kinetics, the absorption change was measured at 771 nm. Typical traces of the absorption change are shown in Figure 5 in a wide time scale in a semilogarithmic representation. At this wavelength, the shift in the electrochrome response of the bacteriopheophytine, Bpheo, absorption can be measured due to the electric field perturbation around the chromophore.[21] Because the logarithmic time window is very wide, it covers 6 orders of magnitude, and both the $P^+Q_A^-Q_B \rightarrow P^+Q_AQ_B^-$ electron transfer and the accompanied reactions (fast phase) and the $P^+(Q_AQ_B)^- \rightarrow PQ_AQ_B$ charge recombination (slow phase) can be followed in a single plot. The kinetic parameters (amplitudes and rate constants) obtained from multiexponential decomposition are summarized in Table 2. Routinely, the time resolution was limited to few tens of microseconds under our conditions, however, for the RC sample bound to the carbon nanotubes, it was somewhat lower, close to 100 μs due to stronger light scattering.

For the RCs sample in the LDAO detergent suspension, the rate of the fastest phase, $k_{AB}(1)_{fast}$, was 13 500 s^{-1}, which was comparable to that reported in the literature for samples with the quinones first depleted then reconstituted.[13,21] A slow component, $k_{AB}(1)_{slow}$, was also resolved. This phase is characteristic of the charge relaxation within the protein induced by the charge separation and the forward electron transfer[21,24] and may reflect the protonation of the characteristic amino acid residues of the protein. It can kinetically limit the overall electron

TABLE 2: Kinetic Parameters of Decomposition of the Absorption Change Kinetics Measured at 771 nm (Figure 5)[a]

	$P^+(Q_AQ_B)^- \rightarrow P(Q_AQ_B)$		$P^+Q_A^- \rightarrow PQ_A$		$(Q_A^-Q_B \rightarrow Q_AQ_B^-)_2$		$(Q_A^-Q_B \rightarrow Q_AQ_B^-)_1$	
771 nm	A_1 (rel)	k_{BP} (s^{-1})	A_2 (rel)	k_{AP} (s^{-1})	A_3 (rel)	$k_{AB}(1)_{slow}$ (s^{-1})	A_4 (rel)	$k_{AB}(1)_{fast}$ (s^{-1})
RC_susp	0.64	0.92	0.20	8.0	0.06	3300	0.10	13500
RC_dried	0.004	0.91	0.75	8.3	0.106	75	0.14	26300
SWNTRC	0.28	0.625	0.62	8.3	0.10	530	n. r.[b]	

[a] RCs of *Rb. sphaeroides* R-26 were incorporated into LDAO detergent micelles (RC_susp), dried on the surface of borosilicate glass (RC_dried), and attached to single-walled nanotubes, then dried on the glass (SWNTRC). *A* and *k* are the relative amplitude (normalized to the total signal) and the rate constants of the components, respectively. The maximum error was smaller than 10%. [b] n. r. = not resolved

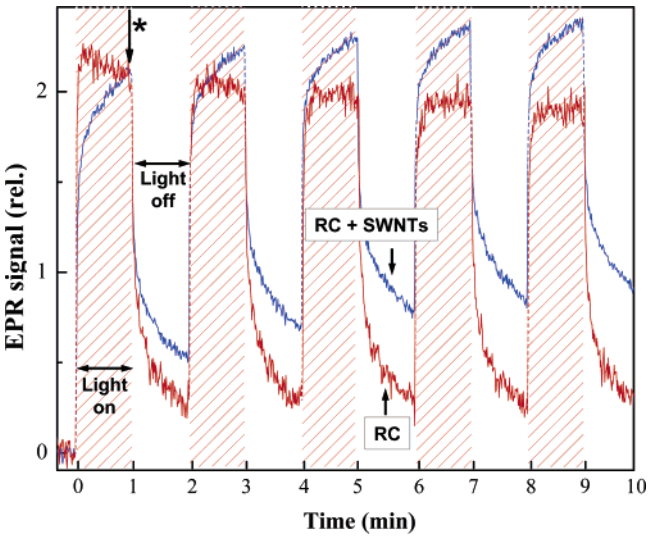

Figure 6. Results of time-resolved EPR experiments performed on both RC and SWNT/RC. The EPR signal was measured and synchronized to the visible light illumination for several on/off runs. There is a clear difference in the response to light between the two samples. (The two samples were normalized to the intensity of the signal at the end of the first illumination period, marked with asterisk.)

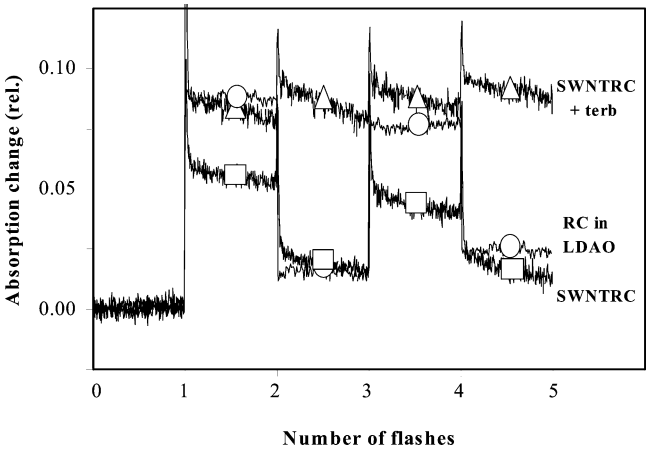

Figure 7. Oscillation of flash-induced absorption changes at 450 nm due to the formation and disappearance of semiquinones in RCs of *Rb. sphaeroides* R-26 attached to SWNT. SWNTRC samples were immersed and rehydrated in a spectroscopic cuvette containing 10 mM TRIS, pH:8.00, 100 mM NaCl, 100 μM ferrocene. The rate of flash repetition was 0.5 Hz. Measurement was taken in the presence (triangles) and in the absence (squeres) of terbutryn. For comparison the oscillation pattern of RCs in LDAO detergent suspension is also indicated (circles). In this later case, the conditions are same, except the flash repetition frequency was 2 Hz.

transport between Q_A^- and Q_B. If the RCs were dried on the glass, $k_{AB}(1)_{fast}$ was found to be similar, $k_{AB}(1)_{fast} = 26\,300\ s^{-1}$, to that in detergent suspension, however, the amplitude increased (Table 2). $k_{AB}(1)_{slow}$, however, shifted to a significantly longer time, from $k_{AB}(1)_{slow} = 3300\ s^{-1}$ to $k_{AB}(1)_{slow} = 75\ s^{-1}$.

In the SWNTRC_dried sample, the very fast component could not be resolved properly under our measuring conditions due to the low signal-to-noise ratio. Nevertheless, a component in the millisecond scale, $k_{AB}(1)_{slow} = 530\ s^{-1}$, was definitely identified that cannot be found in RCs in suspension.

EPR Studies. The small sample quantity for both the RC and SWNT/RC samples did not allow absolute intensity measurements. The two samples were normalized to the intensity of the signal at the end of the first illumination period, asterisked in Figure 6. The two samples show a clear difference in their response to light. The EPR signal changes more gradually both at the on and off edges of the illumination cycles for the SWNT/RC complex than for the RC itself. In our interpretation, this is due to the flow of separated charges from RC to SWNTs and the reverse due to the change in the rate of the interquinone electron transfer in the presence of SWNT. These charges on the carbon nanotubes become EPR silent for an unknown reason. Note that the conduction electron spin resonance in single-walled carbon nanotubes has never been detected following their first reported synthesis.

3.3. Multiple Turnover Studies. In the SWNTRC_dried sample, a slow decay of the oxidized primary donor, P^+, is observed after the single saturating flash excitation. If this is due to the formation of the stable Q_B^-, one would expect a disappearance of the 450 nm absorption change, where semiquinones have light absorption after the second excitation in the presence of suitable exogenous donor to P^+, such as ferrocene. Consequently, RC can perform more turnovers, and the absorption signal exhibits damped binary oscillation after repetitive flash excitation. Because the amplitude of the signal is proportional to the concentration of the semiquinone species (Q_A^- and Q_B^-), the oscillation pattern depends on several factors such as the electron equilibrium (K_{AB}) between the primary and secondary quinones, the quinone exchange between the RC Q_B site and the environment, the proton delivery to the quinones, etc. Figure 7 shows the oscillation of the semiquinone absorption after four successive flash excitations in the SWNT/RC dried sample with and without the electron transport inhibitor, terbutryn. For comparison, the semiquinone signal in the LDAO suspension is also indicated. Figure 7 shows that, in the presence of the nanotube, the oscillation is damped and blocked by the terbutryn. Another important observation is the increase of the signal in the presence of the inhibitor by a factor of about one and the half to four.

4. Discussion

In several interesting works, the coupling of electron transport and protein dynamics was the subject.[25,26] The appearance of a long-lived component was shown in $P^+Q^- \rightarrow PQ$ recombination kinetics, e.g., after continuous illumination,[27] freezing under illumination,[28] treatment with physiologically important phospholipids,[20] or introducing mutations.[28] In our work, light-induced electron-transfer characteristics were measured and compared in RCs dried on a glass surface either bound or

unbound to single-walled carbon nanotubes in order to get a closer look at the RC/carbon nanotube interaction.

Optical and EPR spectroscopy experiments were carried out to see if there is a link between the redox components of the photosynthetic reaction centers and the delocalized π-electron system of the carbon nanotubes. Two approaches could be considered. From the point of view of the nanotubes, it is important to know whether they are able to bind functionally to the protein. If so, that would be an important step forward to several applications, e.g., in light-driven microelectronical, analytical, or energy storage devices.

From the point of view of the reaction center, on the other hand, it is fascinating to learn how the redox properties, i.e., the kinetics and energetics of the cofactors, are influenced by the nanotube. The kinetics and thermodynamics of the observed electron-transfer steps are all sensitive to the environmental factors.[20,29] The rate of the first[21] and the second electron transfer is larger in ethylene glycol than in detergent. In contrast, the charge recombination from the $P^+Q_B^-$ is slowed in this environment.

The degree of freedom of the movements of amino acid side chains of membrane proteins is larger in the native environment.[20] Specific molecules (e.g., phospholipids, like phosphatidylcholine, phosphatidylglycerol, and cardiolipine) that bind to specific sites of the RCs can modify the physical parameters of the charge stabilization.[13,30]

4.1. The Energetics of the Q_B Site. By measuring the kinetics of the flash-induced absorption change, it is possible to follow the redox states of the electron transport components. The charge recombination kinetics measured at 430 and 860 nm did not differ significantly in the detergent; however, there was a more considerable difference in the dried samples. The interpretation of the signal at 430 nm is more complex. Some contribution of the change in the BChl, Bpheo, and quinone absorption due to redox transitions and electrochromic responses cannot be excluded. Because the absorption change at 860 nm is clearly characteristic of the P^+/P redox transition, it is possible to use these kinetic parameters for estimating the $\Delta G_{Q_A^-Q_B \rightarrow Q_AQ_B^-}{}^0$ free energy change. The apparent $K_{AB}{}^{app}$ equilibrium constant of the $P^+Q_A^-Q_B \leftrightarrow P^+Q_AQ_B^-$ reaction can be calculated (see Experimental Section), which corresponds to about -57, -53, and -70 meV $\Delta G_{Q_A^-Q_B \rightarrow Q_AQ_B^-}{}^0$ free energy changes in LDAO, RC_dried, and SWNTRC_dried samples, respectively. It is important to note that using the apparent equilibrium constant, $K_{AB}{}^{app}$, to calculate $\Delta G_{Q_A^-Q_B \rightarrow Q_AQ_B^-}{}^0$ has important limitations (e.g., the rate of the quinone exchange is not comparable with that of the $P^+Q_A^-$ charge recombination, the absorption change reflects the redox state of the cofactors, there are no alternative electron transport routes affecting on $K_{AB}{}^{app}$). Further investigations are needed to describe these limitations with the SWNT environment.

It is interesting to note that a similar shift in the rate of the $P^+Q_A^-Q_B \rightarrow P^+Q_AQ_B^-$ electron transfer and the $P^+(Q_AQ_B)^- \rightarrow PQ_AQ_B$ charge recombination was found in the membrane environment.[13] It was concluded that, in the native environment, the structural flexibility of the membrane protein is higher compared to that in detergent, resulting in a larger free energy gap between the $P^+Q_A^-Q_B$ and $P^+Q_AQ_B^-$ states. It is very unlikely that the situation is the same with the SWNT/RC complex dried on the glass surface. Nevertheless, it is reasonable to assume an increase in the activation energy that is required for these processes. A similar increase in the activation energy was reported on RCs dehydrated by addition of 50% ethylene glycol.[21]

4.2. Charge Compensating Protein Relaxation Events. The intrinsic rate of interquinone ET *per se* is very large, and the observed value is limited by much slower conformational processes.[31] Although the theory of the "conformation gated" mechanism is much more complicated (as indicated in the literature) than simply a limitation of Q_A^- to Q_B electron transfer by the conformation state of the molecule,[32−34] depending on the rate-limiting processes, the observed kinetics of interquinone ET can be decomposed into phases of different rate constants of variable contributions (amplitudes). The change in protonation of specific amino acids and water molecules should be accompanied by the change in the hydrogen bonding network and van der Waals contacts between the molecules.

From the contribution of the rates, $k_{AB}(1)_{fast}$ and $k_{AB}(1)_{slow}$, of the absorption kinetics, it is interesting to conclude that drying the RCs on the surface of the glass does not inhibit the first forward electron transfer. After saturating light excitation, the $P^+Q_A^-Q_B \rightarrow P^+Q_AQ_B^-$ electron transfer occurs in every RCs, resulting in the $P^+Q_A^-Q_B \leftrightarrow P^+Q_AQ_B^-$ equilibrium. If the RCs were solubilized in detergent or dried on the glass, we resolved both $k_{AB}(1)_{fast}$ and $k_{AB}(1)_{slow}$ with a good signal-to-noise ratio (Figure 5, Table 2). All of the kinetic parameters in solutions were comparable with those of already reported in the literature. It is interesting that if the RCs were dried on the glass surface, this $P^+Q_A^-Q_B \rightarrow P^+Q_AQ_B^-$ component in the absorption did not disappear, indicating that the forward electron transfer is completed. In this sample, $k_{AB}(1)_{fast}$ increased to 26 300 s^{-1} compared to that measured in solution, $k_{AB}(1)_{fast} = 13\,500\ s^{-1}$. This is accompanied by a much slower charge compensation conformation component, $k_{AB}(1)_{slow} = 75\ s^{-1}$.

In the RCs in detergent suspension, there is a slow component, corresponding to $k_{AB}(1)_{slow} = 3300\ s^{-1}$, which limits the forward electron transport by conformation movements ("conformational gated mechanism").[31] Although, if the SWNT/RC complex was dried on the glass surface, we could not resolve the very fast component due to the large light scattering, we did resolve a very slow component in the millisecond scale $k_{AB}(1)_{slow} = 530\ s^{-1}$. Time-resolved FTIR experiments showed that specific modes of vibration have a similar lifetime if the temperature is decreased to about 5 °C (900 s^{-1}).[34] These authors suggest the possibility of the slow reoxidation of the Q_A^- by an alternative transient redox couple, X, that limits the overall $P^+Q_A^-Q_B \rightarrow P^+Q_AQ_B^-$ electron transfer.

4.3. Electronic Communication between the RCs and SWNTs. The experiments discussed above indicate clearly that the functional integrity of the Q_B site is disrupted if the RC together with the LDAO detergent is dried on the glass and P^+ disappears very quickly due to the fast $P^+Q_A^- \rightarrow PQ_A$ charge recombination. The slow decay of the absorption change after single saturating excitation is indicative of the slow rereduction of the oxidized primary donor, P^+. Several mechanisms can be accounted for this observation. (a) The interquinone electron equilibrium ($K_{AB} = P^+Q_A^-Q_B \leftrightarrow P^+Q_AQ_B^-$) is shifted to the formation of the product, $P^+Q_AQ_B^-$. (b) By using the rates of the charge recombination processes (k_{AP} and k_{BP}), the apparent equilibrium constant, $K_{AB}{}^{app}$, can be calculated (see Experimental Section), which includes the quinone binding equilibrium as well. Because we used a dried sample, it is reasonable to assume that the turnover of quinone binding/unbinding is disrupted. Because the sample was prepared by using a fully reconstituted Q_B site, it is possible that also the rate of the unbinding, k_{off}, is reduced considerably. Both possibilities can be taken into account with great probability with the requirement of strong interaction between the RC protein and the nanotube.

(c) Another possible explanation of the long living P^+ population in the SWNTRC dried sample is the direct electronic communication between the RC cofactors and the carbon nanotubes. Although, this possibility cannot be excluded, and the results of EPR experiments support this idea, further investigations are needed to prove it.

Further evidence for the charge communication between RC and SWNT can be obtained by measuring the appearance and disappearance of the semiquinone absorption after repetitive flash excitation. In the presence of externally added diffusive electron donor to P^+, which is fast enough compared to the rate of the charge recombination (ferrocene, Fec, fulfils this requirement), this equilibrium shifts to the right direction in the reaction scheme: In this reaction scheme, Fec is ferrocene, and

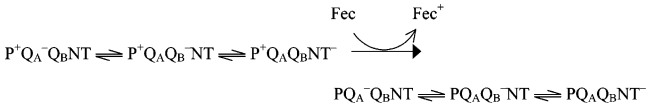

NT is the additional redox component, which contributes to the electron equilibrium; in our model, this can be the SWNT. The general model can be visualized by Figure 1.

After addition of terbutryn, Terb, a specific inhibitor of the Q_B site, the signal amplitude increases and the oscillation disappears because of the increase of the Q_A^- concentration:

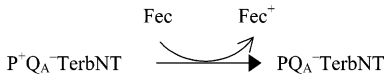

The disappearance of the oscillation alone cannot be explained by the electronic equilibrium between the RC and the nanotubes. Several trivial and nontrivial losses in the electron equilibrium (see above) give similar results. However, the about one and a half to 4-fold increase in the semiquinone signal in the presence of the inhibitor can be explained if there is a third partner in addition to the Q_A^- and Q_B^- sharing the electrons.

Our SWNT/RC samples were prepared by adsorption of RCs on the surface of SWNT physically. The prolonged incubation time allowed RCs to accommodate with almost homogeneous orientation; however, there is no proof until now that this structure is the optimal one. There is already experimental evidence that the electronic communication between the gold surface[35] and carbon electrode[36,37] is highly dependent on the suitable orientation of the binding. Our experiments clearly indicate specific effects on the functioning of RCs in light-induced charge separation and stabilization; nevertheless, further experiments are needed to show the optimal conditions for the orientation.

5. Conclusion

This study provides direct evidence that the integral membrane protein, the photosynthetic reaction center, can be attached to single-walled carbon nanotubes with the apparent binding to specific site(s). Data presented support the idea that one of the effects of carbon tubes includes the stabilization of light-induced charge(s) in photosynthetic energy conversion. The attachment of nanotubes increases the lifetime of the $P^+Q_B^-$ state, probably due to the slow charge recombination between the oxidized primary electron donor, P^+, and negative semiquinone forms, Q_A^- and/or Q_B^-, the reduced primary and secondary quinones, respectively. After the excitation, the intraprotein charge movements are followed by slower reorganization of the protein structure.

The special electronic properties of the SWNT/RC complex open the possible direction of several practical applications, e.g., in microelectronics, analytics, or energy conversion and storage.

Acknowledgment. This work was supported by the Hungarian Science Foundation (OTKA T 048706 and T 046491). The Swiss National Science Foundation and its NCCR "Nanoscale Science" supported the work in Lausanne. Special thanks are due to Professor Gerardo Palazzo, University of Bari, Bari, Italy, for helpful comments and discussions.

References and Notes

(1) Davis, J. J.; Coles, R.; Hill, A. *J. Electroanal. Chem.* **1997**, *440*, 279.
(2) Britto, P. J.; Santhanam, K. S. V.; Ajayan, P. M. *Bioelectrochem. Bioenerg.* **1996**, *41*, 121.
(3) Sotiropoulu, S.; Chaniotakis, A. N. *Anal. Bioanal. Chem.* **2003**, *375*, 103.
(4) Karajanagi, S. S.; Vertegel, A. A.; Kane, R. S.; Dordick, J. S. *Langmuir* **2004**, *20*, 11594.
(5) Sebban, P.; Maróti, P.; Hanson, D. K. *Biochimie* **1995**, *77*, 677.
(6) Allen, J. P.; Williams, J. C. *FEBS Lett.* **1998**, *438*, 5.
(7) Okamura, M. Y.; Paddock, M. L.; Graige, M. S.; Feher, G. *Biochim. Biophys. Acta* **2000**, *1458*, 148.
(8) Paddock, M. L.; Feher, G.; Okamura, M. Y. *FEBS Lett.* **2003**, *555*, 45.
(9) Wraight, C. A. *Biosciences* **2004**, *9*, 309.
(10) Wraight, C. A.; Clayton, R. *Biochim. Biophys. Acta* **1974**, *333*, 246.
(11) McAuley, K. E.; Fyfe, P. K.; Ridge, J. P.; Isaacs, N. W.; Cogdell, R. J.; Jones, M. R. *Proc. Natl. Acad. Sci. U.S.A.* **1999**, *96*, 14706.
(12) Camara-Artigas, A.; Brune, D.; Allen, J. *Proc. Natl. Acad. Sci. U.S.A.* **2002**, *99*, 11055.
(13) Nagy, L.; Milano, F.; Dorogi, M.; Agostiano, A.; Laczko, G.; Szebenyi, K.; Varo, G.; Trotta, M.; Maroti, P. *Biochemistry* **2004**, *43*, 12913.
(14) Milano, F.; Dorogi, M.; Szebényi, K.; Nagy, L.; Maróti, P.; Váró, Gy.; Agostiano, A.; Trotta, M. *Bioelectrochem.* **2006**, in press.
(15) Ormerod, J. G.; Ormerod, K. S.; Gest, H. *Arch. Biochem. Biophys.* **1961**, *94*, 449.
(16) Tandori, J.; Nagy, L.; Puskás, A.; Droppa, M.; Horváth, G.; Maróti, P. *Photosynth. Res.* **1995**, *45*, 135.
(17) Hernadi, K.; Siska, A.; Thien-Nga, L.; Forró, L.; Kiricsi, I. *Solid State Ionics* **2001**, *141*.
(18) Tandori, J.; Nagy, L.; Maróti, P. *Photosynthetica* **1991**, *25*, 159.
(19) Lakatos, M.; Groma, G. I.; Ganea, C.; Lanyi, J. K.; Váró, G. *Biophys. J.* **2002**, *82*, 1687.
(20) Nagy, L.; Fodor, E.; Tandori, J.; Rinyu, L.; Farkas, T. *Austr. J. Plant Physiol.* **1999**, *25*, 465.
(21) Tiede, D. M.; Vázquez, J.; Córdova, J.; Marone, P. *Biochemistry* **1996**, *35*, 10763.
(22) Kleinfeld, D.; Okamura, M. Y.; Feher, G. *Biochim. Biophys. Acta* **1984**, *79*, 1171.
(23) Wraight, C. A.; Stein, R. R. *FEBS Lett.* **1983**, *113*, 73.
(24) Tiede, D. M.; Utschig, L.; Hanson, D. K.; Gallo, D. M. *Photosynth. Res.* **1998**, *55*, 267.
(25) Palazzo, G.; Mallardi, A.; Giustini, M.; Berti, D.; Venturoli, G. *Biophys. J.* **2000**, *79*, 1171.
(26) McMahon, B. H.; Müller, J. D.; Wraight, C. A.; Nienhaus, G. U. *Biophys. J.* **1998**, *74*, 2567.
(27) Kálmán, L.; Maróti, P. *Biochemistry* **1997**, *36*, 15269.
(28) Andrasson, U.; Carlsson, T.; Andreasson, L. E. *Biochim. Biophys. Acta* **2003**, *1607*, 45.
(29) Taly, A.; Baciou, L.; Sebban, P. *FEBS Lett.* **2002**, *532*, 91.
(30) Camara-Artigas, A.; Brune, D.; Allen, J. *Proc. Natl. Acad. Sci. U.S.A.* **2002**, *99*, 11055.
(31) Graige, M. S.; Feher, G.; Okamura, M. Y. *Proc. Natl. Acad. Sci. U.S.A.* **1998**, *95*, 11679.
(32) Breton, J. *Biochemistry* **2004**, *43*, 3318.
(33) Baxter, R. H. G.; Ponomarenko, N.; Srajer, V.; Pahl, R.; Moffat, K.; Norris, J. R. *Proc. Natl. Acad. Sci. U.S.A.* **2004**, *101*, 5982.
(34) Remy, A.; Klaus, G. *Nat. Struct. Biol.* **2003**, *10*, 637.
(35) Trammell, S. A.; Wang, L.; Zullo, J. M.; Shashidar, R.; Lebedev, N. *Biosens. Bioelectron.* **2004**, *19*, 1649.
(36) Trammell, S. A.; Spano, A.; Price, R.; Lebedev, N. *Biosens. Bioelectron.* **2006**, *21*, 1023.
(37) Das, R.; Kiley, P. J.; Segal, M.; Norville, J.; Yu, A.; Wang, L.; Trammell, S. A.; Reddick, L. E.; Kumar, R.; Stellacci, F.; Lebedev, N.; Schnur, J.; Bruce, B. D.; Zhang, S.; Baldo, M. *Nano Lett.* **2004**, *4*, 1079.